Changes of Cd content in chloroplasts are mirrored by the activity of photosystem I, but not by photosystem II

E.A. LYSENKO[+] (iD) and V.V. KUSNETSOV[+] (iD)

Institute of Plant Physiology, Russian Academy of Sciences, Botanicheskaya 35, 127276 Moscow, Russia

Abstract

We searched for a direct Cd action on the photosynthetic electron transport chain using induced chlorophyll fluorescence and P_{700} light absorption. Young barley and maize plants were treated with Cd in concentrations of toxic (80 μM) and nearly lethal (250 μM). The maximal and relative photochemical activities of PSI, its major limitation at the donor side, and partially acceptor-side limitation of PSII changed in agreement with Cd accumulation in the corresponding chloroplasts. Acceptor-side limitation of PSII increased with a direct Cd action at 80 μM that was overcome with an indirect Cd action at 250 μM. These alterations can be explained by Cd/Cu substitution in plastocyanin. The photochemical and nonphotochemical quenching by PSII varied diversely which cannot be explained unambiguously by any mechanism. The limitations of PSI [$Y_{(ND)}$, $Y_{(NA)}$] and PSII (q_C) were compared for the first time. They were ranged: $Y_{(NA)} < q_C < Y_{(ND)}$.

Introduction

Cadmium is a highly toxic heavy metal distributed all over the world (Pan *et al.* 2010, Zou *et al.* 2021) – sources of Cd accumulation range from natural (*e.g.*, volcanic activity) to industrial and agricultural origin. Mineral fertilizer applications, as well as mining and smelting, are considered to be the major sources of Cd input into the environment (Bigalke *et al.* 2017, Kumar *et al.* 2021). Moreover, Cd mobility is very high under natural conditions (Gaillardet *et al.* 2003, Jigyasu *et al.* 2020). Many water sources demonstrated relatively high Cd content which is hazardous for both plants and animals (Mahajan *et al.* 2022).

Plants possess multiple protective mechanisms against Cd toxicity (Seregin and Ivanov 2001, Lin and Aarts 2012), however, these mechanisms are mostly energy-dependent. The photosynthetic electron-transport chain in

Highlights

- PSI activity changed in agreement with the changes of Cd content in chloroplasts
- The data on PSII activity cannot be clearly explained by Cd action
- PSI changes can be explained by Cd/Cu substitution in plastocyanin

thylakoidal membranes is the primary site of energy input into a plant organism. Therefore, protecting chloroplasts against Cd toxicity is of high importance. Most terrestrial plants restrict Cd movements from roots to leaves (Baker 1981). A small amount of Cd is introduced to chloroplasts (Baryla *et al.* 2001, Pietrini *et al.* 2003, Lysenko *et al.* 2015); *in vivo*, Cd content in chloroplasts varied from 4.5 to 336 ng mg^{-1}(Chl) and from 0.02 to 14.3% of all Cd in leaves (*see* Lysenko *et al.* 2015). Inside chloroplasts, Cd is concentrated in thylakoids; in barley thylakoids, the content of Cd is sufficient to inhibit some components of the electron-transport chain (Lysenko *et al.* 2019).

Plant biologists have been analyzing Cd's impact on the photosynthetic electron-transport chain for decades. At present, we have two major problems in this area. First, there is a controversy about Cd's impact on the processes around the PSII. In many studies, Cd treatment did not change the ratio F_v/F_m of PSII (Burzyński and Żurek 2007, Shi and Cai 2008, Lysenko *et al.* 2015); however, the fall of F_v/F_m was also demonstrated (Dias *et al.* 2013). The photochemical coefficients were more sensitive to Cd action. The Cd treatment decreased both Φ_{PSII} [synonym $Y_{(II)}$] and q_P (Ci *et al.* 2010) or only one of them (Burzyński and Żurek 2007, Lysenko *et al.* 2020) while the coefficient $X_{(II)}$ increased (Lysenko *et al.* 2020). Cd treatment influenced neither Φ_{PSII} nor q_P in Zn/Cd hyperaccumulator plants (Tang *et al.* 2013). Nonphotochemical quenching by PSII increased (He *et al.* 2008), unchanged (Burzyński and Żurek 2007), or decreased (Lysenko *et al.* 2015, 2020) by Cd treatment.

Second, the changes observed can be caused by either direct or indirect Cd action. Discriminating between direct and indirect mechanisms of Cd action is the fundamental question. The PSI activity and Cd accumulation inside chloroplasts are only rarely analyzed.

We have found a model to distinguish between direct and indirect action of Cd on processes in chloroplasts (Lysenko *et al.* 2015). For maize and barley plants, the concentration of 80 μM CdSO$_4$ was inhibitory and far from lethal; the concentration of 250 μM CdSO$_4$ was very poisonous and even lethal in the prolonged experiment (Klaus *et al.* 2013, Lysenko *et al.* 2015). Consequently, elevating Cd concentration should gradually increase numerous indirect effects in both species.

In chloroplasts, Cd content is small and limits a direct Cd action because any target exceeds Cd in its number (reviewed in Lysenko *et al.* 2019). Therefore, we can use Cd content in chloroplasts as a measure to estimate its direct action in these chloroplasts. At 80 μM CdSO$_4$, the maize plants accumulated a small amount of Cd in chloroplasts [49 ± 5 ng mg^{-1}(Chl)]; at 250 μM CdSO$_4$, the maize plants acquired more Cd in the chloroplasts [92 ± 20 ng mg^{-1}(Chl)] (Lysenko *et al.* 2015). The barley plants showed an unexpected pattern of Cd accumulation. At 80 μM CdSO$_4$, the barley plants accumulated a large amount of Cd in the chloroplasts [171 ± 26 ng mg^{-1}(Chl)]. At 250 μM CdSO$_4$, Cd content in the barley chloroplasts did not increase further [126 ± 7 ng mg^{-1}(Chl)]; it decreased while the decrease was insignificant (Lysenko *et al.* 2015). We suggest that a direct Cd effect on processes in

the photosynthetic electron-transport chain should follow Cd accumulation in the chloroplasts. A direct Cd effect in maize should be small at 80 μM Cd and further increase at 250 μM Cd. In barley, a direct Cd effect should be large at 80 μM Cd with no further increase at 250 μM Cd.

Previously, we revealed two unusual effects in barley plants. *In vivo*, Cd treatment increased the level of "closed" PSII and reduced the photochemical activity of PSI more than the photochemical activity of PSII; these effects were specific to Cd (Lysenko *et al.* 2020). The model described above allows us to investigate whether these effects can be referred to as a direct or an indirect Cd action. The finding of a potential Cd direct effect should benefit our understanding of Cd action inside chloroplasts.

The present study was performed according to the previous experiment that defined Cd content in the chloroplasts (Lysenko *et al.* 2015). Barley and maize plants were treated with 80 μM and 250 μM CdSO$_4$ for six days; nine-day-old plants were analyzed with the use of pulse amplitude modulation (PAM) technique. The chlorophyll (Chl) *a* fluorescence and P$_{700}$ light absorption were investigated with both induction curves (IC) and rapid light curves (RLC) methods. The thorough analysis of PSII and PSI activities *in vivo* is presented below.

Materials and methods

Plant growth conditions: Barley (*Hordeum vulgare* L. cv. Luch) and maize (*Zea mays* L. cv. Luchistaya) seedlings were grown in phytotron chambers at 21°C (barley) or 25–26°C (maize), 180–220 μmol(photon) m^{-2} s^{-1} and a photoperiod of 16-h light/8-h dark under continuous aeration on modified Hoagland medium (Lysenko *et al.* 2019). Preliminary, caryopses were kept for 2–3 days at 4°C on a filter paper moistened with 0.25 mM CaCl$_2$; imbibed caryopses were germinated in the growth conditions. Two-day-old seedlings were transferred to vessels with Hoagland medium. The next day, CdSO$_4$ was added to the hydroponic media to the final concentrations of 80 μM or 250 μM. Simultaneously, an independent experiment with Cu- and Fe-treatment was performed using the same experimental design; some data from this unpublished experiment were used to show the specificity of Cd action in two figures below. In this experiment, CuSO$_4$ was added to the final concentration of 80 μM; FeSO$_4$ was added to the final concentration of 1.5 mM. The analyses were performed on nine-day-old seedlings. For more details *see* Lysenko *et al.* (2015, 2019, 2020).

PAM analysis: The Chl *a* fluorescence and P$_{700}$ light absorption were simultaneously registered with the *Dual-PAM-100* (*Walz*, Germany). The largest fully developed leaf was used for the measurement: the first leaf of barley and the second leaf of maize. Chl *a* fluorescence was measured from the adaxial side of leaves. The Chl *a* fluorescence was excited at 460 nm [Int. #5, 12 μmol(photon) m^{-2} s^{-1}; the measuring light]. P$_{700}$ is the reaction center chlorophyll of PSI; the level of oxidized P$_{700}$ was measured as the difference in light absorption at

830 and 875 nm (Int. #5). The red light of 635 nm was used as the actinic light (AL) and for the saturation pulses (SPs).

The plants were adapted in the dark for 30 min, transferred rapidly to the *Dual-PAM-100*, avoiding bright light, and kept in the dark for another 4 min. In the dark, the measuring light only was used for the determination of minimal (F_0) Chl fluorescence; the first SP [4 mmol(photon) m^{-2} s^{-1}, 500 ms] was applied for the measurement of maximal (F_m) Chl fluorescence; the pre-illumination with far-red light [720 nm, Int. #10, ~250 μmol(photon) m^{-2} s^{-1}, Pfündel *et al.* 2013] followed with the second SP were employed for the determination of minimal (P_0) and maximal (P_m) P_{700} absorption. The measurement of basic parameters in the dark-adapted state was followed with the extra 30 s of darkness.

Next, AL [128 μmol(photon) m^{-2} s^{-1}] was turned on; IC was measured for 7.5 min. The first SP was applied after 0.5 s since AL induction; then, SPs were applied every 40 s. The maximum level of fluorescence in the light (F_m') and maximal P_{700} change in the light (P_m') were measured during SP; the stationary fluorescence (F_s, synonym F) and P_{700} light absorption (P) were measured just before SP (Pfündel *et al.* 2013). After SP, the illumination was switched to the far-red light [720 nm, Int. #10, ~250 μmol(photon) m^{-2} s^{-1}, Pfündel *et al.* 2013] for 5 s and the minimum level of fluorescence in the light (F_0') was determined. The minimal level of P_{700} light absorption (P_0) was measured after cessation of far-red light both in the dark and light regimes (Klughammer and Schreiber 1994, 2008).

The method IC is the correct and, probably, preferable way of plant adaptation to light conditions before an application of the RLC method (Lysenko 2021). After the completing IC, the method RLC was started in 6 s. In RLC, each step of AL lasted for 30 s; the set of AL intensities is shown in the figures. The other parameters were the same as in IC.

The parameters of P_{700} light absorption were calculated as follows: $Y_{(I)} = (P_m' - P)/(P_m - P_0)$; $Y_{(ND)} = (P - P_0)/(P_m - P_0)$; $Y_{(NA)} = (P_m - P_m')/(P_m - P_0)$; $Y_{(I)} + Y_{(ND)} + Y_{(NA)} = 1$ (Klughammer and Schreiber 1994, 2008).

The parameters of Chl fluorescence were calculated using the following equations: $F_v = F_m - F_0$; $F_v' = F_m' - F_0'$; $\Phi_{PSII} = (F_m' - F_s)/F_m'$ (Genty *et al.* 1989, Kalaji *et al.* 2014); $q_P = (F_m' - F_s)/F_v'$, $q_N = (F_v - F_v')/F_v$ (Schreiber *et al.* 1986, van Kooten and Snel 1990); $X_{(II)} = (F_m' - F_s)/F_v$, $q_C = (F_s - F_0')/F_v$ (Lysenko *et al.* 2020); NPQ $= (F_m - F_m')/F_m'$ (Bilger and Björkman 1990); $q_N + X_{(II)} + q_C = 1$ (Lysenko *et al.* 2020).

Calculation of ratios between Chl fluorescence and P_{700} absorption: We calculated the ratios between the photochemical activities of both photosystems [$Y_{(I)}/X_{(II)}$] (Lysenko *et al.* 2020) and between their limitations [$q_C/Y_{(NA)}$ and $q_C/Y_{(ND)}$]. In some cases, the values of q_C, $Y_{(NA)}$, and $Y_{(ND)}$ were very small. In case when such a small value occurs in the denominator of the ratio then it should be removed. The zero values must be discarded because it is forbidden to divide by zero. The negative values have

to be discarded because dividing by a negative number generates a nonsense value. The tiny positive values originated extremely high ratios; a single enormous ratio is capable of distorting a mean of 20–30 normal ratios by several times. For the last case, we have established the criteria for eliminating these data points.

A small signal comparable to a baseline fluctuation can be computed as negative, zero, or extremely small positive. Therefore, the values of denominators [$Y_{(NA)}$ and $Y_{(ND)}$] were considered. Values q_C are frequently low; therefore, q_C was used as a numerator. Denominator values ≤ 0.025 can be discarded when they are outside of relatively continuous distribution. Denominator values $0.025 < X > 0.030$ can be discarded a) if their ratios were 2 times higher than the largest point of relatively continuous distribution or b) if their ratios were 1.8 times higher than the largest point of relatively continuous distribution, however, removal of this single data point decreased standard error (SE) at least by one third. Denominator values ≥ 0.030 can be discarded a) if their ratios were 3 times higher than the largest point of relatively continuous distribution or b) if their ratios were 2.5 times higher than the largest point of relatively continuous distribution, however, removal of this single data point decreased SE at least by one half. Some suspicious data points can not be discarded according to these criteria; they can prevent the elimination of larger, apparently false ratios. One or two "irremovable" data points were considered outliers; three "irremovable" data points were considered as an edge of relatively continuous distribution. These threshold criteria have been selected empirically. The $q_C/Y_{(ND)}$ data points were discarded at the beginning of curves only [40 s in IC, AL 72 and 97 μmol(photon) m^{-2} s^{-1} in RLC]. The $q_C/Y_{(NA)}$ data points were discarded from any part of the curves; if half or more of the data points were removed from a curve then this curve was discarded completely. The portion of data points discarded was relatively small; in a single point, half of the data points were removed.

The values $Y_{(I)}$ and $X_{(II)}$ demonstrated stable ratios; seven denominator data points were removed from the data set. At the beginning of IC (AL 0.5 s) and the final of RLC [AL 1,954 μmol(photon) m^{-2} s^{-1}], the level of $X_{(II)}$ is very low; the values $X_{(II)} \leq 0.005$ in barley and $X_{(II)} \leq 0.001$ in maize were discarded.

The general map of the data points discarded is represented in Tables 1S–3S (*supplement*).

Statistics: Control plants and plants treated with 80 μM Cd were studied in three independent experiments. Because of greater variability under nearly lethal conditions of 250 μM Cd, plants were studied in four complete independent experiments; for barley plants, IC was measured in two more experiments. The numbers of plants measured with the methods "Darkness+IC/RLC" were as follows: barley 17/17 in control, 17/17 at 80 μM Cd, and 37/21 at 250 μM Cd; maize 18/18 in control, 18/18 at 80 μM Cd, and 24/19 at 250 μM Cd. Additional treatment with 80 μM Cu and 1.5 mM Fe was performed in six independent experiments; IC was measured in 36 and 37

barley plants correspondingly. The data were processed using the *Excel* (*Microsoft*) software. The significance of differences between mean values was verified using the two-tailed *Student*'s *t*-test, $p \leq 0.05$.

Results

Maximal Chl fluorescence and P_{700} absorption in darkness: Parameters measured in the dark-adapted state showed maximal activities of the photosystems with no limitations; they therefore reflected the quantitative levels of both photosystems. The barley plants demonstrated a gradual decline of all the parameters of Chl fluorescence: F_m, F_v, F_0, and F_v/F_m (Fig. 1); the decrease was only significant at 250 µM Cd. In contrast, P_{700} light absorption changed in agreement with Cd content in the chloroplasts. At 80 µM Cd, both P_m and P_m/F_v decreased substantially; the larger concentration of 250 µM Cd enlarged neither Cd content in the chloroplasts (Lysenko *et al.* 2015), nor Cd effect on P_m and P_m/F_v (Fig. 1*D,F*).

Maize plants demonstrated a gradual decline of F_m, F_v, and P_m (Fig. 1); it was under both general toxicity of Cd and its accumulation in maize chloroplasts (Klaus *et al.* 2013, Lysenko *et al.* 2015). At 250 µM Cd, the ratio P_m/F_v showed a larger decline of P_m compared with F_v

(Fig. 1*F*). The minimal Chl fluorescence demonstrated unusual changes. At 80 µM Cd, the F_0 level increased; at 250 µM Cd, the level of F_0 returned to the control level (Fig. 1*C*). The changes of F_0 altered F_v/F_m dynamics. In maize, F_v/F_m dropped at 80 µM Cd with no further decrease at 250 µM Cd (Fig. 1*E*).

Chl fluorescence under light conditions: The dynamics of photochemical quenching of light energy by PSII are shown in Fig. 2. The time immediately after light induction (0.5 s) is the only point at which changes in PSII activity were proportional to Cd accumulation in the chloroplasts of both species. The values of $X_{(II)}$ after 0.5-s AL are shown in Fig. 1S*C* (*supplement*) with a higher resolution; the values of q_P and Φ_{PSII} demonstrated the same tendency at this point.

The coefficient $X_{(II)}$ indicates the portion of photochemically active PSII in current light conditions ($F_m' - F_s$) compared with the maximal level (F_v). In barley plants, Cd treatment did not reduce the portion of photochemically active PSII (Fig. 2*A,C*). The photochemical coefficient q_P shows the balance between open ($F_m' - F_s$) and closed ($F_s - F_0'$) PSII in current light conditions. The cadmium treatment significantly decreased the level of q_P (Fig. 2*E,G*); however, it was achieved by increasing
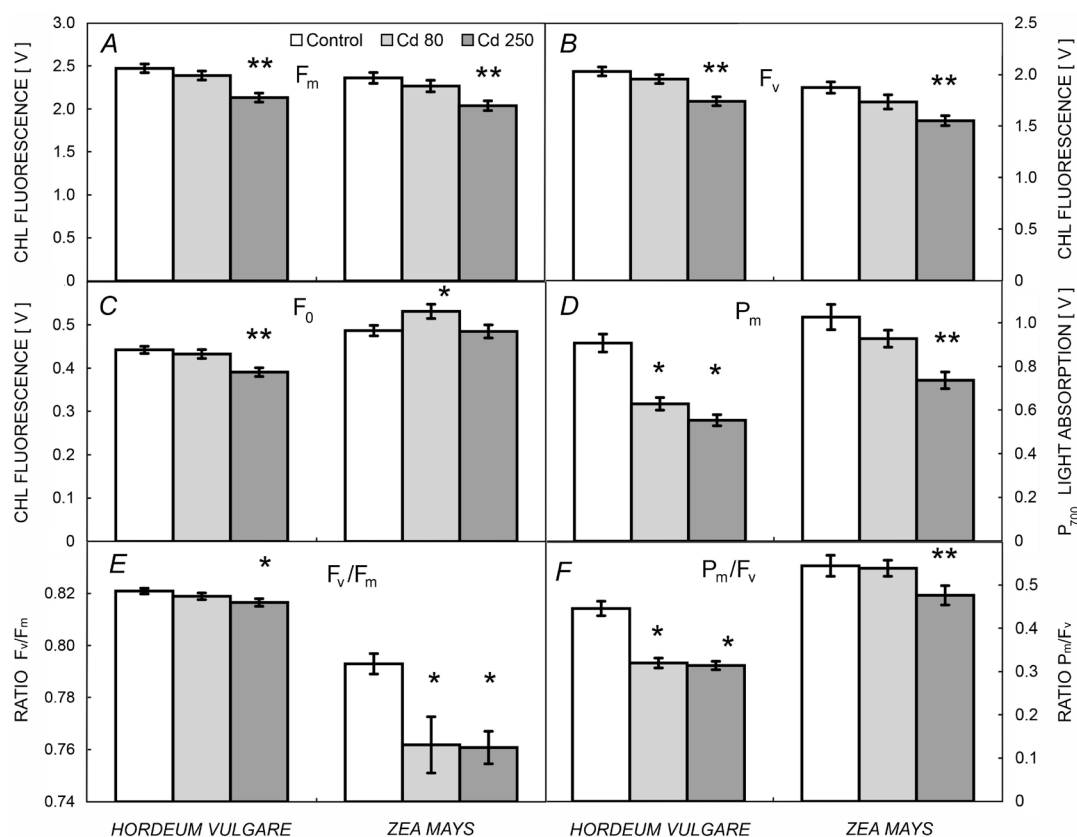
Fig. 1. Basic photosynthetic values in the dark-adapted plants. (*A*) Maximal Chl fluorescence in darkness (F_m); (*B*) variable Chl fluorescence in darkness (F_v); (*C*) minimal Chl fluorescence in darkness (F_0); (*D*) maximal P_{700} change in darkness (P_m); (*E*) maximal quantum yield of PSII (F_v/F_m); (*F*) ratio P_m/F_v in darkness. Bars represent the variants of treatment: white – control, light grey – Cd 80 µM, dark grey – Cd 250 µM. Data are presented as means ± SE. * – the difference from the control is significant at $p \leq 0.05$. ** – the difference between both control and Cd 80 µM is significant at $p \leq 0.05$.
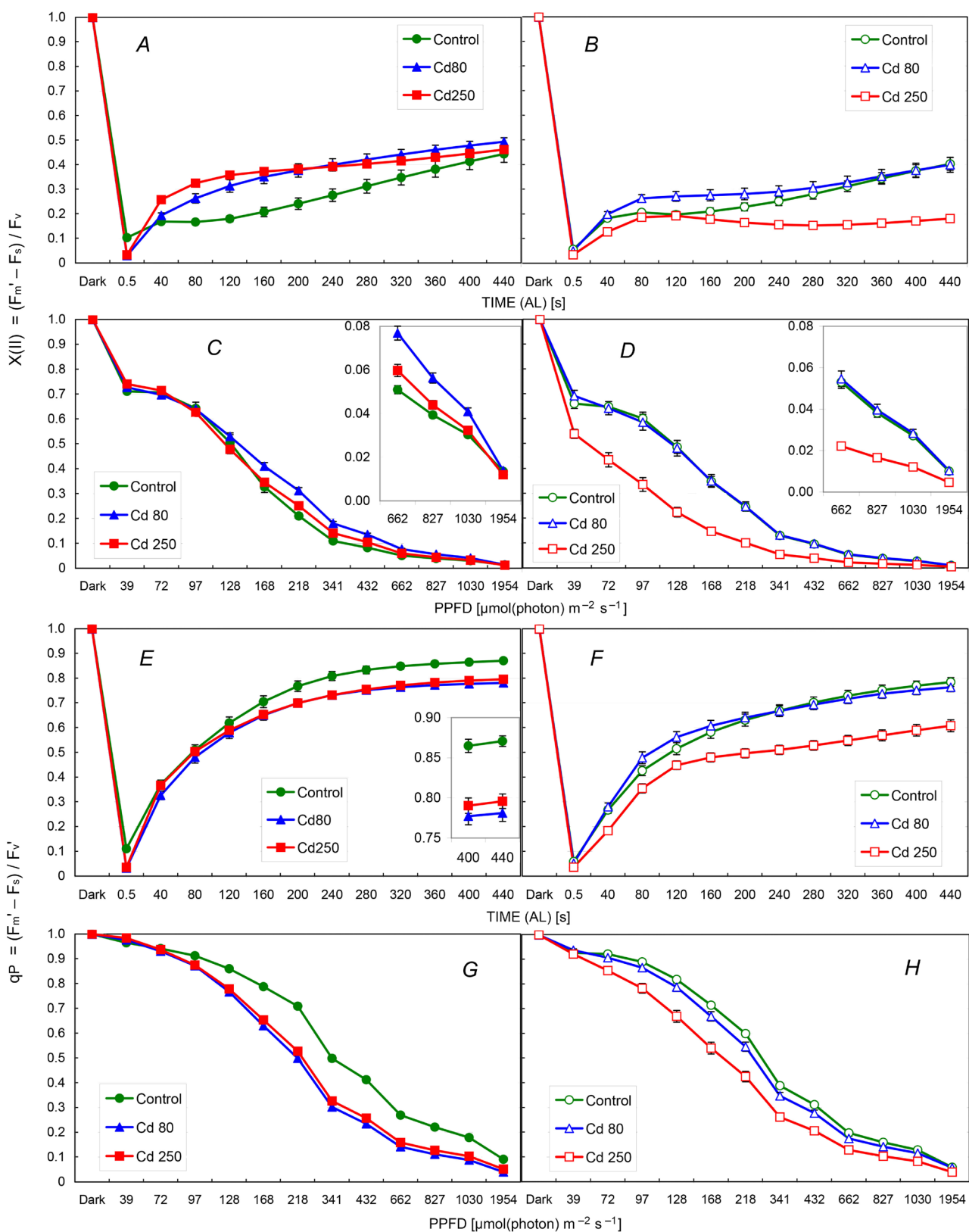
Fig. 2. Dynamics of photochemical coefficients $X_{(II)}$ and q_P of PSII. (*A–D*) $X_{(II)}$; (*E–H*) q_P (dynamics of Φ_{PSII} are represented in Fig. 2S). (*A,B,E,F*) Induction curves (IC); (*C,D,G,H*) rapid light curves (RLC). Lines represent the variants of treatment: *green circles* – control, *blue triangles* – Cd 80 μM, *red squares* – Cd 250 μM. *Filled symbols* represent barley; *open symbols* represent maize. AL – actinic light. Data are presented as means ± SE. The insets show the corresponding values with the higher resolution.

the portion of closed PSII (q_C, *see* below) that was proportionally larger than the increase of open PSII. The coefficient Φ_{PSII} demonstrated an intermediate tendency (Fig. 2S*A,C*; *supplement*).

In maize, the photochemical activity of PSII varied following Cd accumulation in the chloroplasts (Lysenko *et al.* 2015). At 80 µM Cd, the photochemical quenching was mostly unchanged. At 250 µM Cd, the photochemical quenching decreased substantially. All the coefficients $X_{(II)}$ (Fig. 2*B,D*), q_P (Fig. 2*F,H*), and Φ_{PSII} (Fig. 2S*B,D*) showed the same tendency.

Nonphotochemical energy quenching is the major way to reduce the photochemical quenching of PSII. In barley, Cd treatment reduced nonphotochemical quenching (Fig 3*A,C*). In IC, both 80 µM and 250 µM Cd decreased nonphotochemical quenching similarly (Fig. 3*A*). In RLC, 80 µM Cd decreased nonphotochemical quenching more than 250 µM Cd (Fig. 3*C*). Both coefficients q_N (Fig. 3*A,C*) and NPQ (Fig. 3S*A,C*; *supplement*) demonstrated the same tendencies.

In maize, 80 µM Cd mainly unchanged nonphotochemical quenching (Fig. 3*B,D*). The small significant decreases were found in the middle of IC (80–200 s, Fig. 3*B*, Fig. 3S*B*) and at the end of RLC [AL of 827–1030 µmol(photon) m^{-2} s^{-1}, Fig. 3*B*; AL of 662–1954 µmol(photon) m^{-2} s^{-1}, Fig. 3S*B*]. At 250 µM Cd, nonphotochemical quenching increased in maize (Fig. 3*B,D*; Fig. 3S*B,D*). Thus, Cd treatment induced the opposite changes of nonphotochemical quenching in barley and maize.

Light energy, which was neither photochemically nor nonphotochemically quenched, is retained in closed PSII complexes. The portion of closed PSII (q_C) is represented in Fig. 4. In barley, Cd treatment increased the portion of closed PSII. In IC, both 80 µM and 250 µM Cd imposed small and equal effects (Fig. 4*A*). In RLC, we revealed a high level of the closed PSII at 80 µM Cd; at 250 µM Cd, the increase was moderate (Fig. 4*C*).

In maize, Cd imposed little effect on q_C dynamics. The method IC demonstrated no influence of Cd treatment (Fig. 4*B*). The method RLC revealed small bidirectional changes of q_C (Fig. 4*D*). At 80 µM Cd, the portion of closed PSII was above the control level; at 250 µM Cd, the portion of closed PSII was below the control level. Thus, RLC dynamics revealed the similarity between barley and maize. In both species, elevating the concentration from 80 µM Cd to 250 µM Cd stimulated the increase of q_N (Fig. 3*B,D*) and decrease of q_C (Fig. 4*B,D*).

P_{700} light absorption under light conditions: The dark-adapted plants showed substantial values of $Y_{(I)}$; they were higher in maize than in barley (Fig. 5*A,B*; Fig. 1S*A*). Cd treatment decreased $Y_{(I)}$-in-darkness in maize and increased it in barley (Fig. 1S*A*).

Under illumination, the photochemical activity of PSI showed a reasonable correlation with Cd accumulation
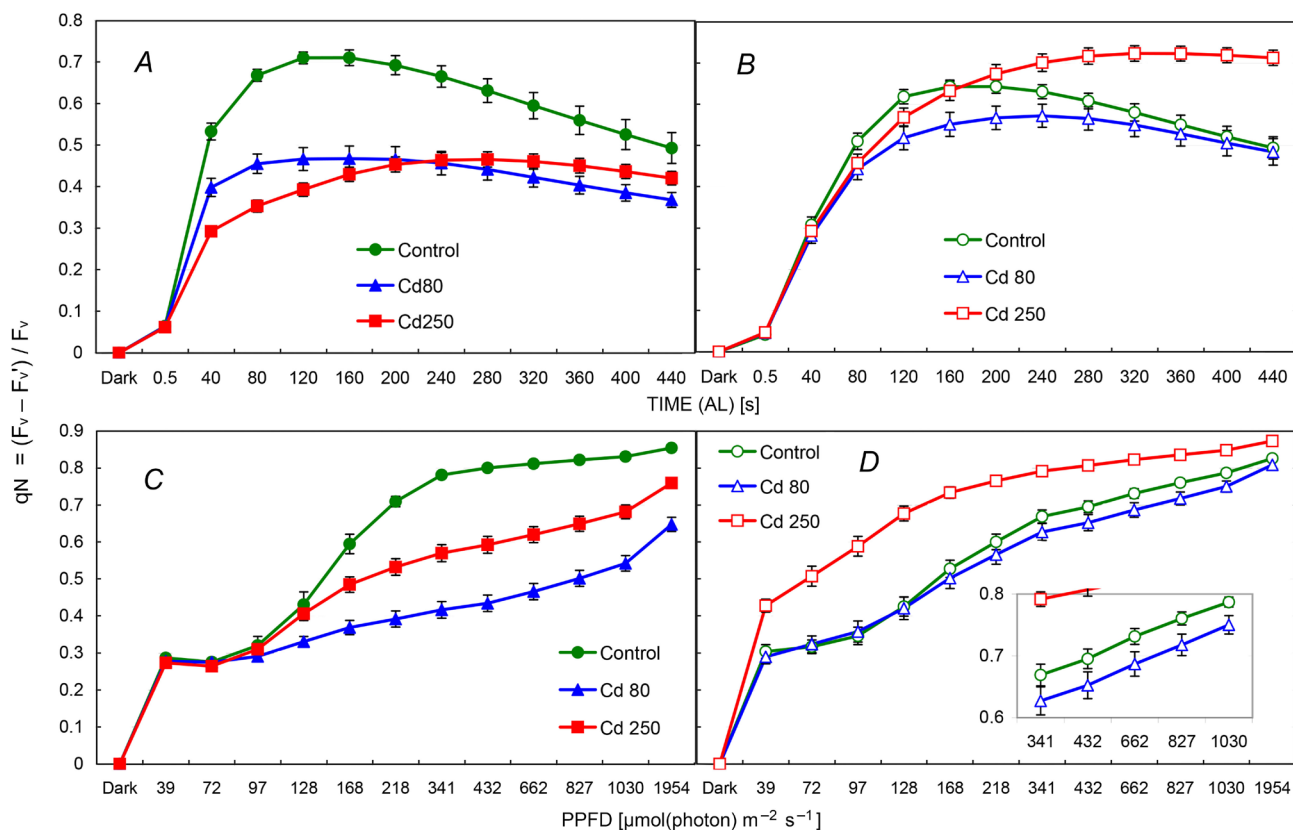
Fig. 3. Dynamics of nonphotochemical quenching (q_N) of PSII. (*A,B*) Induction curves (IC); (*C,D*) rapid light curves (RLC). All other designations are the same as in Fig. 2. Dynamics of NPQ are represented in Fig. 3S.

Fig. 4. Dynamics of closed PSII (q_C). (*A,B*) Induction curves (IC); (*C,D*) rapid light curves (RLC). All other designations are the same as in Fig. 2.
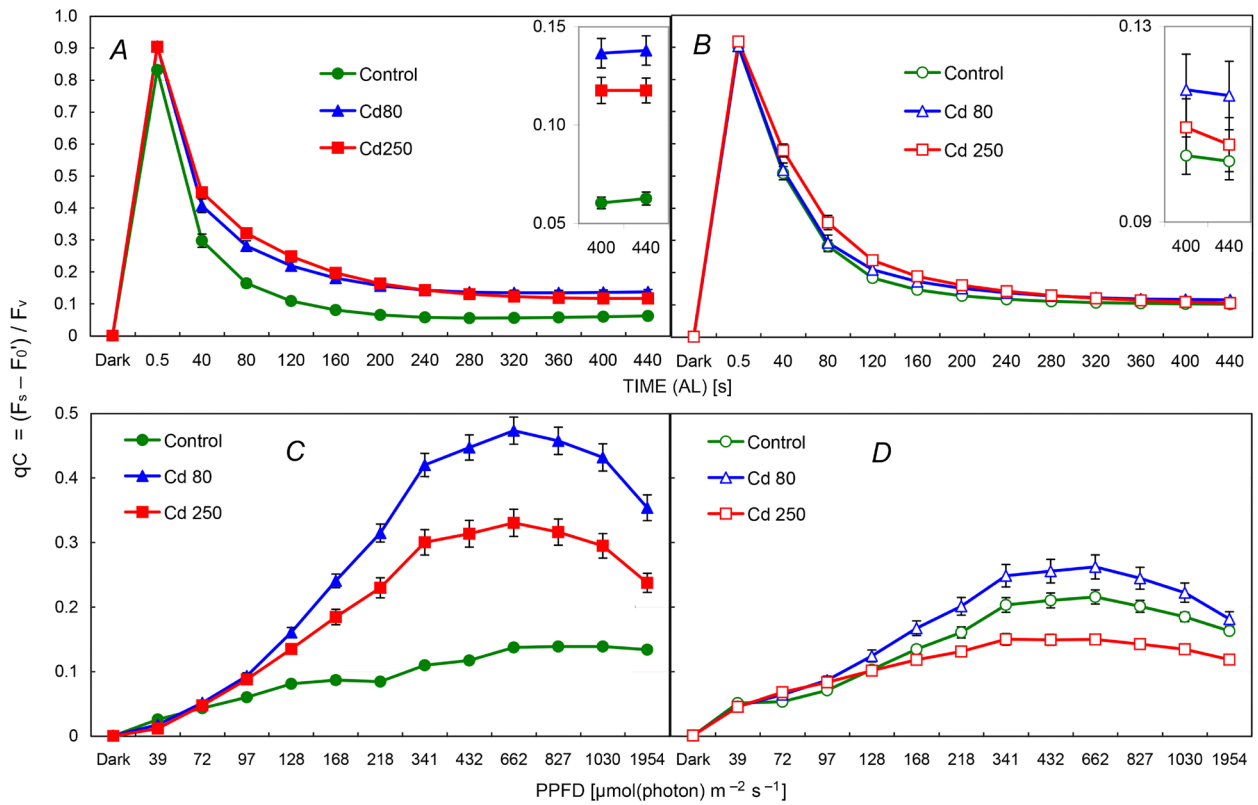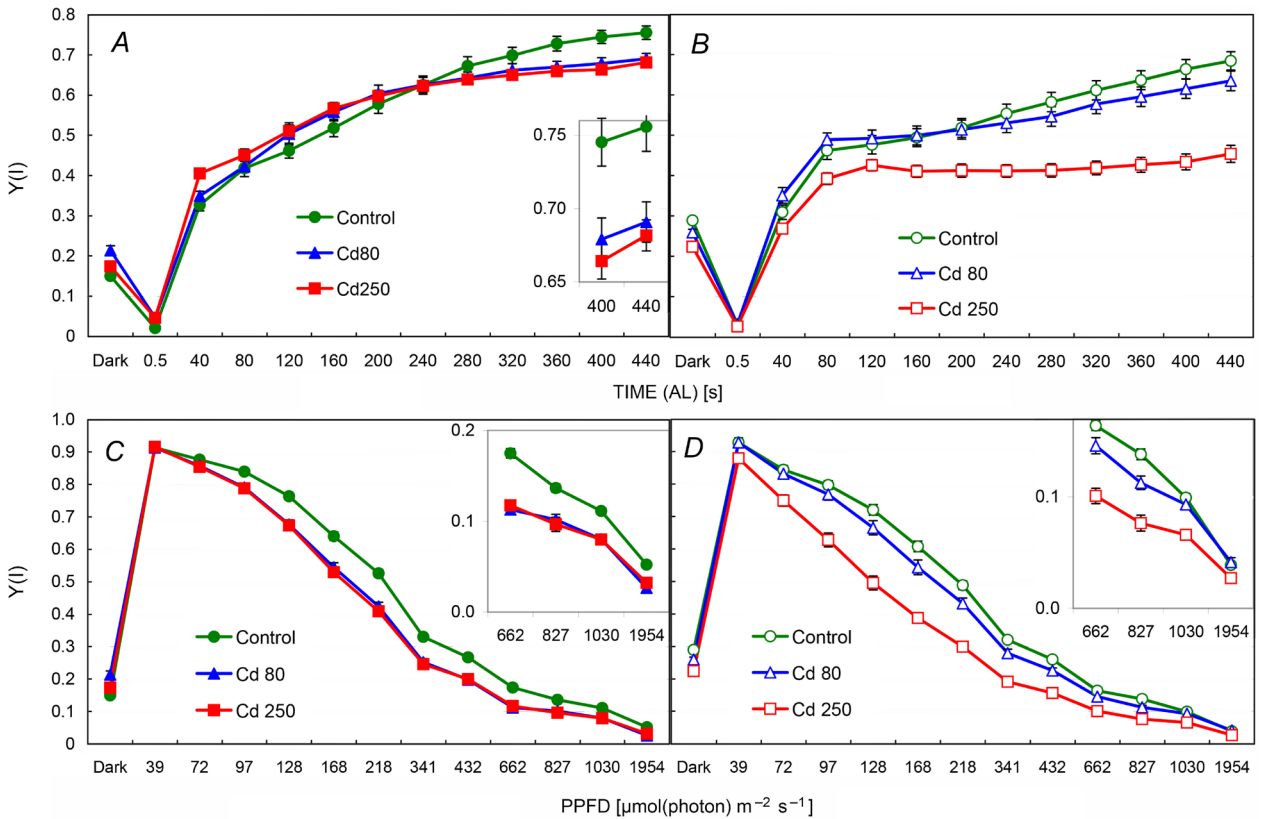

Fig. 5. Dynamics of the quantum yield $Y_{(I)}$ of PSI. (*A,B*) Induction curves (IC); (*C,D*) rapid light curves (RLC). All other designations are the same as in Fig. 2.

in the chloroplasts. In barley, 80 μM Cd and 250 μM Cd induced the same decrease of $Y_{(I)}$ (Fig. 5*A,C*); the differences from the control were significant in IC from 360/320 s and in RLC from AL of 97/72 μmol(photon) $m^{-2} s^{-1}$ (for the concentrations 80/250 μM Cd, respectively). In maize, 80 μM Cd imposed no (IC) or very small (RLC) decrease of $Y_{(I)}$ [significant at AL of 168–827 μmol(photon) $m^{-2} s^{-1}$]. At 250 μM Cd, $Y_{(I)}$ was substantially reduced in maize (Fig. 5*B,D*).

The photochemical activity of PSI was limited mostly at the donor side (Fig. 6). Donor-side limitation of $Y_{(ND)}$ reached its maximal level in 1–2 min after the light induction and then declined slowly in most cases (Fig. 6*A,B*). In barley, Cd treatment accelerated this process; the same maximal level of $Y_{(ND)}$ was reached and began to decline 40 s earlier than in the control (Fig. 6*A*). However, $Y_{(ND)}$ relaxed slower in Cd-treated plants than in the control; at the end of IC, the near stationary level of $Y_{(ND)}$ increased in Cd-treated plants (significant from 360 or 400 s). In RLC, $Y_{(ND)}$ was increased in all the range of AL intensities; the increase was significant in all but one point (Fig. 6*C*). The effect of 80 μM and 250 μM Cd was equal (Fig. 6*A,C*). In maize, 80 μM Cd induced a minor increase of $Y_{(ND)}$ while 250 μM Cd induced a larger increase of $Y_{(ND)}$; the control, 80 μM Cd, and 250 μM Cd differed significantly from each other throughout both IC and RLC (Fig. 6*B,D*).

The impact of the acceptor-side limitation of $Y_{(NA)}$ was small (Fig. 6*E–H*), while it increased slowly along with the increase of AL intensity (Fig. 6*G,H*). Solely at 0.5 s after the light induction, $Y_{(NA)}$ was great and restricted the photochemical activity of PSI (Fig. 6*E,F*).

Ratios of PSII and PSI activities: The photochemical activities of PSI and PSII can be compared with the use of ratio $Y_{(I)}/X_{(II)}$ (Lysenko *et al.* 2020). In the control, both plant species demonstrated similar dynamics of $Y_{(I)}/X_{(II)}$ in IC (Fig. 7*A,B*) and RLC (Fig. 7*C,D*; Fig. 5S, *supplement*). In barley, Cd treatment decreased the ratio $Y_{(I)}/X_{(II)}$; this means that the balance of photosystems was shifted in favor of PSII. The effect of 250 μM Cd was smaller than the effect of 80 μM Cd (Fig. 7*A,C*). The effect of Cd was dissimilar to the effects of other heavy metals, namely Cu and Fe (Fig. 7*A*). In maize, the treatment with 80 μM Cd imposed no or small decrease of $Y_{(I)}/X_{(II)}$ [80–200 s in IC, AL of 662–827 μmol(photon) $m^{-2} s^{-1}$ in RLC]. On the contrary, the treatment with 250 μM Cd increased the ratio $Y_{(I)}/X_{(II)}$ (Fig. 7*B,D*).

The coefficients q_C, $Y_{(ND)}$, and $Y_{(NA)}$ are calculated similarly; each of them shows which part of the maximal photochemical ability (F_v or P_m) was lost due to a particular limitation. The ratio $q_C/Y_{(NA)}$ enables comparing limitations at the acceptor sides of PSII and PSI correspondingly. The acceptor side of PSI is limited mostly by the activity of the Calvin–Benson cycle; the acceptor side of PSII is limited by most of the electron-transfer chain. So, the ratio $q_C/Y_{(NA)}$ enables comparing limitations of the electron-transfer chain and the Calvin–Benson cycle. Some points in dynamics were excluded from the analysis. In the darkness, $Y_{(NA)}$ is zero and q_C is close to zero which

makes the analysis impossible and meaningless. In RLC, at the first AL intensity, too many $Y_{(NA)}$ data points should be discarded (*see* Materials and methods) making the averages questionable.

Immediately (0.5 s) after the light induction, both acceptor-side limitations were high and their ratios were close to 1 (Fig. 8*A,B*); in barley, both limitations were equalized by Cd treatment. The ratio reached the peak and then declined. In Cd-treated plants, the peak was reached in 80 s (barley) or 80–120 s (maize). In control barley plants, the peak was reached later (120 s); control maize plants demonstrated no peak (Fig. 8*A,B*). At AL of 128 μmol(photon) $m^{-2} s^{-1}$, control plants reached the steady-state level of about 1, therefore, the limitations were equal. Cadmium treatment increased $q_C/Y_{(NA)}$ values; the steady-state level was close to 2 (Fig. 8*A,B*). The latter means that q_C was two times larger than $Y_{(NA)}$. In RLC, under the diverse AL intensities, $q_C/Y_{(NA)}$ was > 1 usually; control plants demonstrated low values of $q_C/Y_{(NA)}$ under low AL intensities (Fig. 8*C,D*). Generally, $q_C/Y_{(NA)}$ dynamics mirrored the dynamics of q_C (Fig. 4); probably, the only exception was the time slot of 0.5 s since the light induction.

The ratio $q_C/Y_{(ND)}$ enables comparing limitations in the section of the electron-transport chain between the acceptor side of PSII and the donor side of PSI. Some points in dynamics were excluded from the analysis. q_C is nearly zero in darkness and $Y_{(ND)}$ is zero at 0.5 s after the light induction; the analysis of these points is senseless. In the beginning of RLC, control plants and also Cu- and Fe-treated plants (not shown) demonstrated too many $Y_{(NA)}$ data points that should be discarded (*see* Materials and methods) making the averages questionable. Therefore, we excluded the point AL of 39 μmol(photon) $m^{-2} s^{-1}$ from the analysis.

In the beginning of IC, the ratio $q_C/Y_{(ND)}$ exceeded 1; control barley plants also demonstrated $q_C/Y_{(ND)}$ > 1 in the beginning of RLC (Fig. 8*E–H*). In these cases, the limitation at the acceptor side of PSII (q_C) prevailed. The rest of the dynamics showed $q_C/Y_{(ND)}$ < 1 (Fig. 8*E–H*); therefore, the limitation at the acceptor side of PSII was mostly smaller than the limitation at the donor side of PSI. In barley, Cd treatment increased the ratios $q_C/Y_{(ND)}$ (Fig. 8*E,G*). In maize, 80 μM Cd decreased $q_C/Y_{(ND)}$ slightly while 250 μM Cd decreased $q_C/Y_{(ND)}$ obviously (Fig. 8*F,H*).

We revisualized $q_C/Y_{(ND)}$ dynamics in Fig. 6S (*supplement*). All $q_C/Y_{(ND)}$ dynamics decreased to a quasi-stationary level that was kept for 1–2 min. In a variant (species/Cd concentration), this level was the same in both IC and RLC with a single exception; values of quasi-stationary levels varied from 0.2 to 0.65 (Fig. 6S). Next, $q_C/Y_{(ND)}$ increased in IC and decreased in RLC. In IC, the higher the Cd concentration, the smaller the increase; generally, this increase was larger in barley than in maize (Fig. 6S). In RLC, the higher the quasi-stationary level, the larger the subsequent decrease (Fig. 6S). Cd treatment increased the short-time stabilization level in barley, while decreasing it in maize (Fig. 6S).
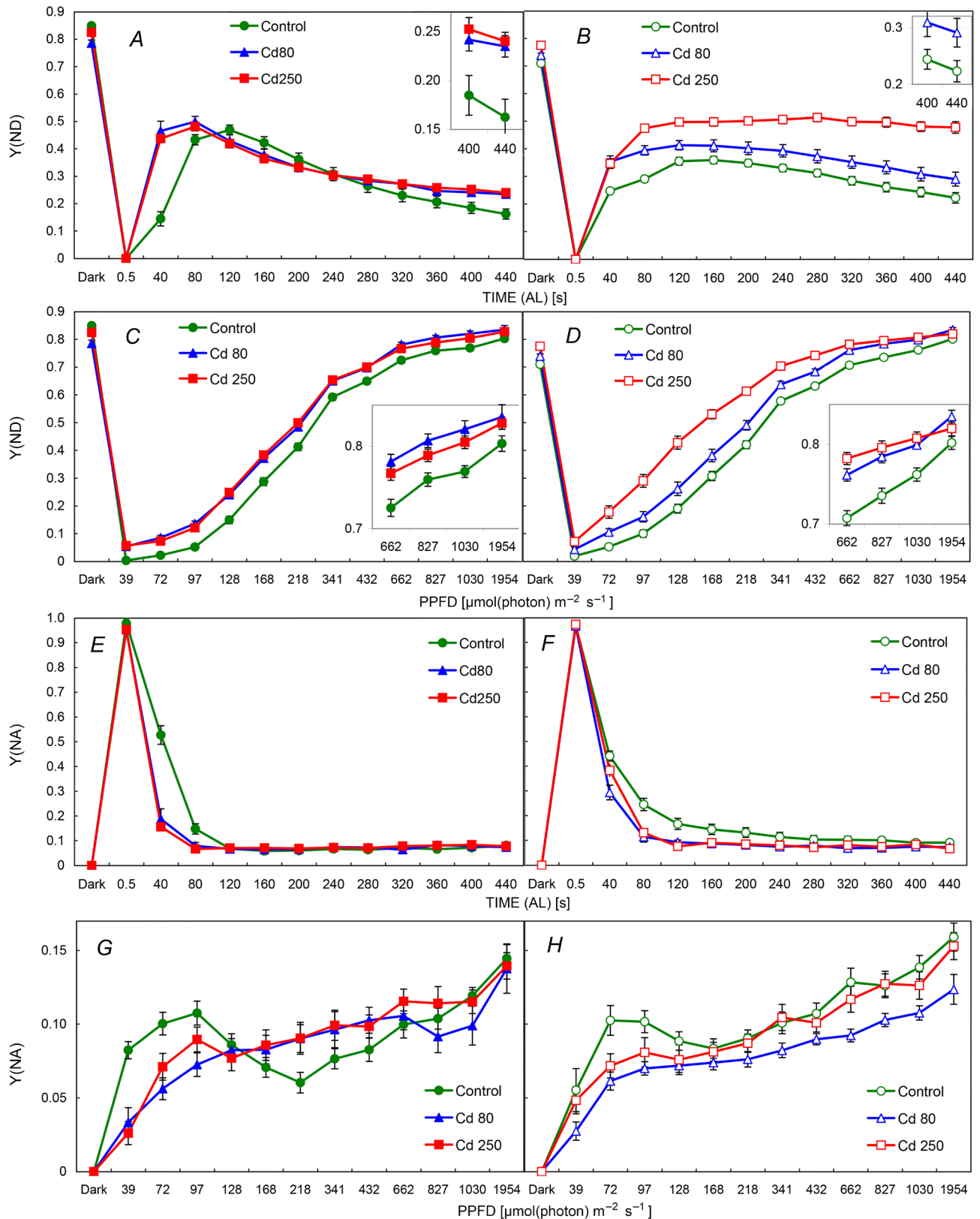
Fig. 6. Dynamics of the limitations of PSI. (*A–D*) limitation at the donor side, $Y_{(ND)}$; (*E–H*) limitation at the acceptor side, $Y_{(NA)}$. (*A,B,E,F*) Induction curves (IC); (*C,D,G,H*) rapid light curves (RLC). All other designations are the same as in Fig. 2.
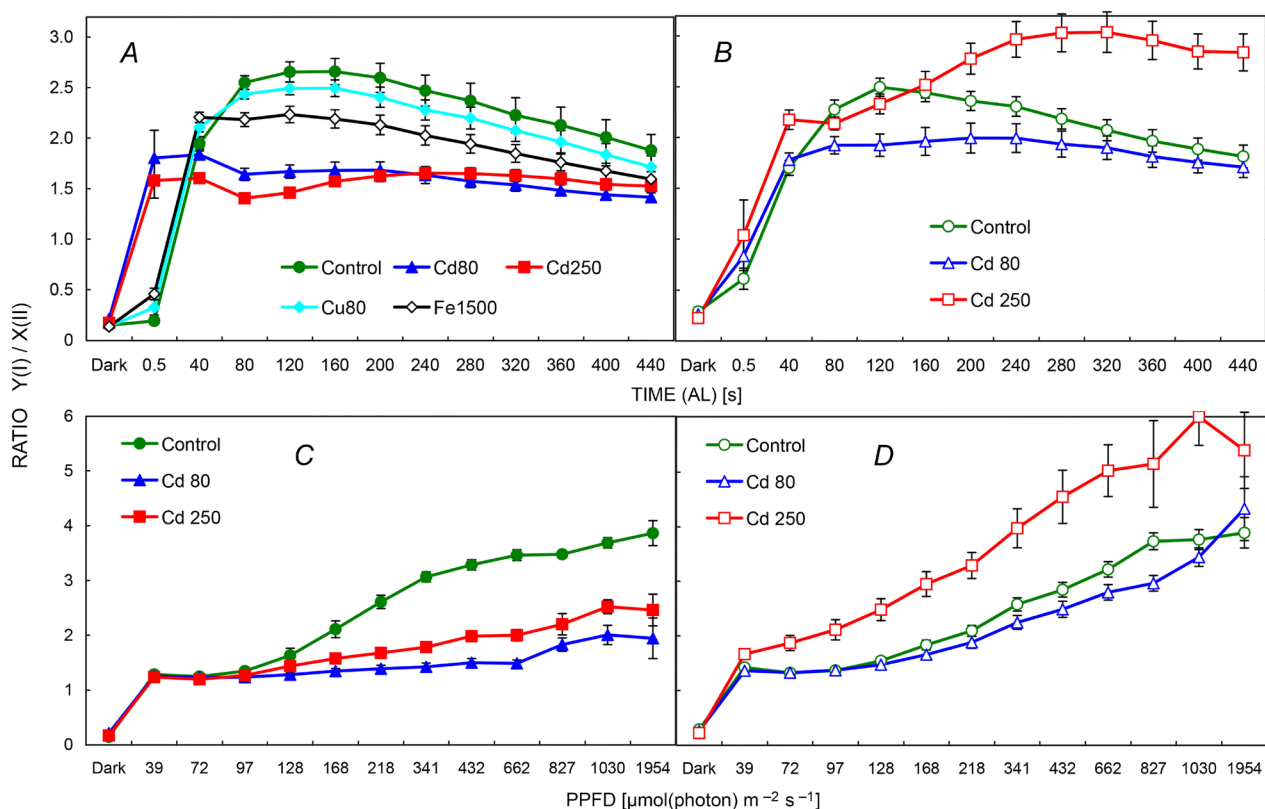
Fig. 7. The ratio $Y_{(I)}/X_{(II)}$ showing balance between the photochemical activities of PSI and PSII. (*A,B*) Induction curves (IC); (*C,D*) rapid light curves (RLC). Lines with *diamond symbols* (*A*) represent additional variants of treatment: *turquoise filled* – Cu 80 µM, *black open* – Fe 1,500 µM. All other designations are the same as in Fig. 2.

Discussion

We used the model of two Poaceae species with different patterns of Cd accumulation in the chloroplasts (Lysenko *et al.* 2015). We applied this model to distinguish between the direct and indirect effects of Cd on the processes in the electron-transport chain in chloroplasts. An indirect effect should reflect the general toxicity and be increased along with the increase of Cd concentration in hydroponics; this increase should be similar in both species (Klaus *et al.* 2013, Lysenko *et al.* 2015). A direct effect should reflect Cd content in the chloroplasts (Lysenko *et al.* 2015). At 80 µM Cd, a direct effect should be small in maize and large(r) in barley. At 250 µM Cd, a direct effect should be increased in maize and show no further increase in barley.

Maximal parameters in darkness: Adapting to darkness is applied to reduce any limitation of the photochemical activities of PSII and PSI; the parameters measured in the dark-adapted state reflect quantities of functionally active reaction centers of PSII (Chl fluorescence) and PSI (P_{700} light absorption).

The parameters of Chl fluorescence (F_m, F_v, F_0, F_v/F_m) demonstrated a gradual decline along with the growth of Cd content in mineral media (Fig. 1). In maize, F_0 changed nonlinearly (Fig. 1*C*), which correspondingly influenced

F_v/F_m alteration (Fig. 1*E*).

The maximal change of P_{700} (P_m) altered in agreement with Cd content in the chloroplasts (Fig. 1*D*). Probably, the gradual slope of F_m and F_v reflected just a reduction of leaf size and/or chloroplast density in these leaves. So, normalized P_m (P_m/F_v) showed better agreement with Cd content in the chloroplasts. In barley, P_m/F_v was significantly reduced at 80 µM Cd with no more reduction at 250 µM Cd; in maize, P_m/F_v remained unchanged at 80 µM Cd and decreased at 250 µM Cd (Fig. 1*F*).

The larger decrease in P_m than in F_v was specific to Cd stress. Cu treatment decreased P_m/F_v to a lesser extent, Fe treatment unchanged it (Lysenko *et al.* 2020), and heat stress increased P_m/F_v in barley and maize plants of the same age (Lysenko *et al.* 2023).

These data suggest that the quantity of functionally active PSII was diminished with an indirect action of Cd, while the reduction of functionally active PSI can be explained by a direct Cd action in the chloroplasts.

PSI activity under illumination: The dynamics of P_{700} parameters changed in agreement with Cd accumulation in the chloroplasts (Lysenko *et al.* 2015). In barley, the quantum yield of PSI $Y_{(I)}$ decreased moderately at 80 µM with no further reduction at 250 µM (Fig. 5*A,C*). In maize, $Y_{(I)}$ slightly decreased at 80 µM Cd and showed a large decrease at 250 µM Cd (Fig. 5*B,D*).

The decrease in PSI photochemical quenching was
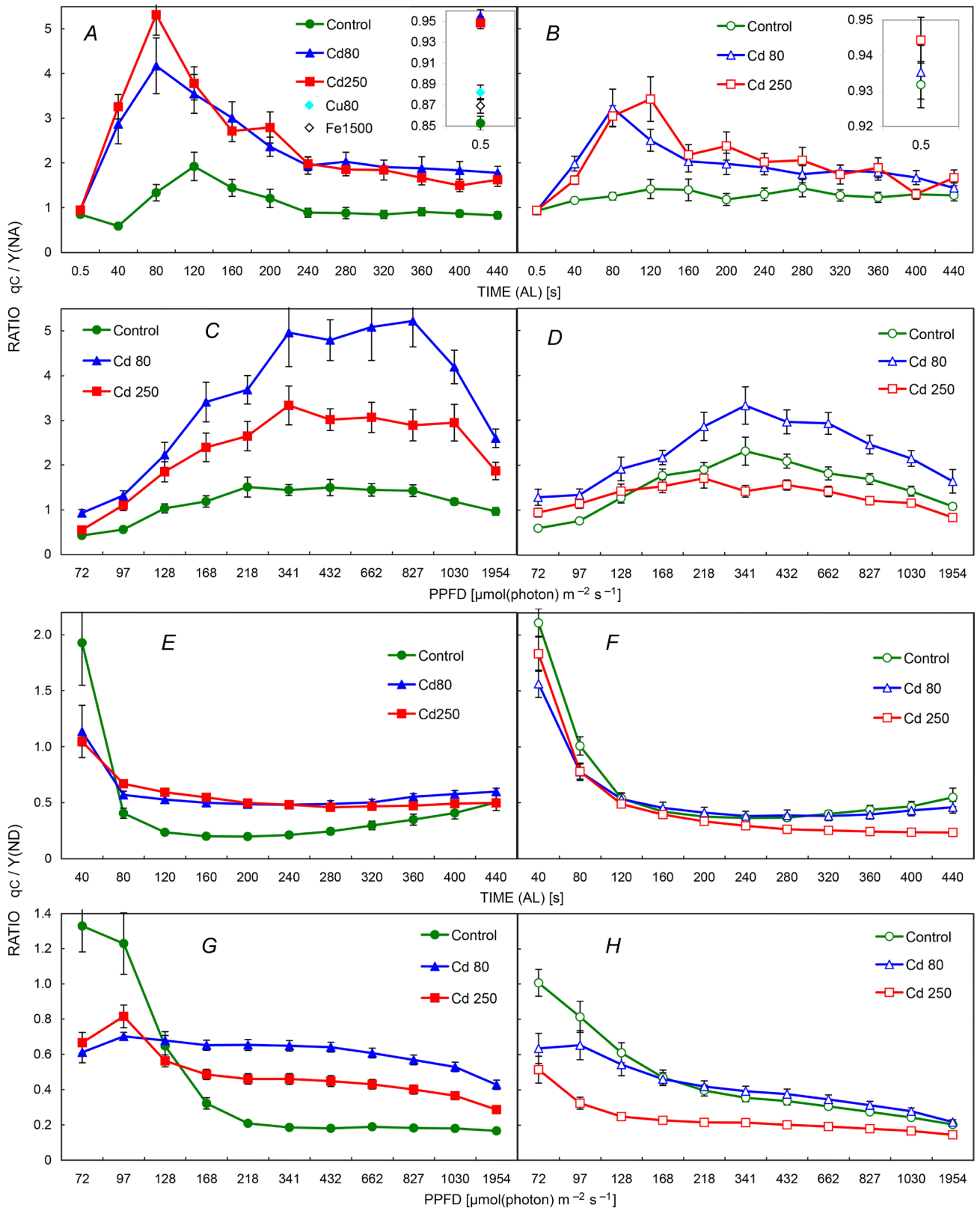
Fig. 8. The ratios showing balance of limitations between the acceptor side of PSII (q_C) and the acceptor [$Y_{(NA)}$] or donor [$Y_{(ND)}$] sides of PSI. (A–D) ratios $q_C/Y_{(NA)}$; (E–H) ratios $q_C/Y_{(ND)}$. (A,B,E,F) Induction curves (IC); (C,D,G,H) rapid light curves (RLC). All other designations are the same as in Figs. 2 and 7.

caused by an increasing limitation at the donor side [$Y_{(ND)}$]. In barley, $Y_{(ND)}$ increased equally at both 80 μM and 250 μM Cd; this increase was observed at the end of IC and all over RLC (Fig. 6A,C). In maize, 80 μM Cd caused a small increase of $Y_{(ND)}$ while 250 μM Cd induced a large increase of $Y_{(ND)}$ (Fig. 6B,D). The increase of $Y_{(ND)}$ was rather specific to Cd. The excess of Cu also increased $Y_{(ND)}$ while the excess of Fe did not increase $Y_{(ND)}$ (Lysenko *et al.* 2020); the heat stress decreased $Y_{(ND)}$ in nine-day-old barley and maize plants (Lysenko, unpublished data).

The limitation of PSI at the acceptor side $Y_{(NA)}$ was small and showed no correlation with Cd content in the chloroplasts (Fig. 6E–H).

Thus, we observed the relationship between Cd content in the chloroplasts and Cd effect on PSI. At 80 μM Cd, maize chloroplasts accumulated a small amount of Cd [49 ± 5 ng mg^{-1}(Chl)]; in this condition, PSI activity was not influenced at all (P_m/F_v) or significantly [P_m, $Y_{(I)}$] whereas its limitation $Y_{(ND)}$ slightly increased. At 250 μM Cd, maize chloroplasts accumulated more Cd [92 ± 20 ng mg^{-1}(Chl)] (Lysenko *et al.* 2015); this magnification was significant at $p = 0.0754$ only. However, it was followed by the large significant inhibition of PSI [P_m, P_m/F_v, $Y_{(I)}$] and increasing donor-side limitation [$Y_{(ND)}$] of PSI. More probably, Cd content was increased in the maize chloroplasts at 250 μM Cd comparing with 80 μM Cd; yet, more than four repeats of the experiment were required to fit into $p<0.05$. We observed higher accumulation of Cd in the first and second leaves of maize at 250 μM Cd than at 80 μM Cd; however, each time the difference was insignificant. It was observed in two independent studies with the same experimental design (Klaus *et al.* 2013, Lysenko *et al.* 2015) and with prolonged treatment (Klaus *et al.* 2013); in the latter case, the difference was significant for the third leaves solely (leaves of upper storeys accumulated Cd equally). At 250 μM Cd, maize plants were severely damaged and 42% died in a one-month treatment. This increased their biological variability; in some cases, we had to repeat simple experiments with leaves 10–12 times (Klaus *et al.* 2013).

At 80 μM Cd, barley chloroplasts accumulated a large amount of Cd [171 ± 26 ng mg^{-1} (Chl)]. At 250 μM Cd, barley chloroplasts accumulated less Cd [126 ± 7 ng mg^{-1}(Chl)]; the decrease was insignificant (Lysenko *et al.* 2015). At both 80 μM and 250 μM Cd, the activity of PSI decreased equally [P_m/F_v, $Y_{(I)}$] or the difference was insignificant (P_m); donor-side limitation $Y_{(ND)}$ increased equally as well. Up to this, we considered that both Cd content in the chloroplasts and Cd effect on PSI was not increased at 250 μM compared with 80 μM Cd; it is true. However, whether the equal effect on PSI was induced by equal or even a smaller content of Cd at 250 μM comparing with 80 μM Cd?

There are several possible explanations. First, we can assume both contents are equal using the insignificance of the difference as the key reason. But it does not seem reliable. In the leaves of barley plants, Cd content decreased at 250 μM compared with 80 μM Cd; the decrease was significant and substantial (Lysenko *et al.* 2015). The decrease of Cd content in the leaves practically

unchanged the proportion of Cd introduced into the chloroplasts. The current experimental design with 80 μM Cd and barley is the advantageous model; we used it in a series of studies. At 80 μM Cd, barley chloroplasts accumulated 237 ± 30 ng Cd mg^{-1}(Chl) (Lysenko *et al.* 2019) and 214 ± 22 ng Cd mg^{-1}(Chl) (Lysenko *et al.* 2020); both values were significantly higher than 126 ± 7 ng Cd mg^{-1}(Chl) accumulated at 250 μM Cd (Lysenko *et al.* 2015). One more treatment was one day shorter; eight-day-old barley plants accumulated in the chloroplasts 152 ± 6 ng Cd mg^{-1}(Chl) ($n = 10$) (Lysenko *et al.*, unpublished data) that was also significantly higher than 126 ± 7 ng Cd mg^{-1}(Chl). In another study, barley chloroplasts accumulated the same amount of Cd [125 ± 6 ng mg^{-1}(Chl), $n = 8$] (Lysenko *et al.*, unpublished data); however, one parameter of experimental design was changed in this experiment and that can influence Cd accumulation. More probably, barley plants accumulated less Cd in both leaves and chloroplasts at 250 μM Cd than at 80 μM Cd.

Second, we can admit that though Cd contents in the chloroplasts were different, but the difference was too small and/or exceeded a threshold level; therefore, the same direct effect was imposed both at 80 μM and at 250 μM Cd. Third, we can suppose that the Cd direct effect was also smaller at 250 μM Cd; however, it was supplemented by an indirect Cd effect; therefore, the entire effects were equal at both 80 μM and 250 μM Cd. We regard the latter explanation as more probable. Both barley and maize plants were reduced much more at 250 μM compared with 80 μM Cd; the higher general toxicity should increase numerous indirect effects in both species. In maize, a direct Cd effect on PSI could also be supplemented by an indirect effect; however, we cannot distinguish it within the framework of this experimental model. The interaction of direct and indirect effects is discussed below considering the changes of closed PSII reaction centers.

The analyses of PSI activity under Cd stress are scarce. *In vitro*, Cd treatment did not affect PSI activity (Bazzaz and Govindjee 1974). *In vivo*, Cd treatment inhibited PSI activity at the acceptor side in 21-day-old maize plants (Siedlecka and Baszyński 1993). In barley chloroplasts, Cd was concentrated in thylakoids; the quantity of Cd was sufficient to replace Cu in plastocyanin (Lysenko *et al.* 2019). Cd-substituted plastocyanin is routinely used in analytical studies as a variant incapable of performing electron transfer (*e.g.*, Díaz-Moreno *et al.* 2005). The hypothesis of Cd/Cu substitution in plastocyanin can explain the mechanism of direct inhibition of PSI at the donor side (Figs. 1, 5, 6) and its correspondence with the changes of Cd content in the chloroplasts (Lysenko *et al.* 2015).

Two more features should be mentioned. In the darkness, $Y_{(I)}$ was higher in maize than in barley which could be attributed to the higher impact of cyclic electron transport around PSI in C_4 plants (Fig. 1SA). In barley, Cd treatment increased $Y_{(I)}$ in the dark. In maize, Cd treatment gradually decreased $Y_{(I)}$ in the dark; though, it remained higher than in barley. Recently, we have revealed that $Y_{(I)}$

in the dark increased with heat stress in both barley and maize (Lysenko *et al.* 2023). Presumably, these species can increase an electron donation from stromal reductants to PSI (Havaux 1996, Yamane *et al.* 2000, Rumeau *et al.* 2007); however, this ability was inhibited by Cd treatment in maize.

In barley plants, Cd stress accelerated PSI readaptation to the light conditions. Cd-treated plants reached the maximum and started a relaxation of $Y_{(ND)}$ faster than control plants (Fig. 6*A*). At the beginning of IC, Cd treatment decreased $Y_{(NA)}$ faster than in the control (Fig. 6*E*). In barley plants under tolerated heat stress, $Y_{(I)}$ reached the steady-state level earlier than in the control barley plants (Lysenko *et al.* 2023). In maize plants, such acceleration was absent (Fig. 6*B*), smaller (Fig. 6*F*), or not so obvious (Lysenko *et al.* 2023).

Dynamics of Chl fluorescence under illumination: The dynamics of Chl fluorescence represented the complex interplay between the photochemical quenching (Fig. 2), nonphotochemical quenching (Fig. 3), and a portion of closed PSII complexes (Fig. 4) that was influenced by species-specific features. The corresponding coefficients – $X_{(II)}$, q_N, and q_C – are comparable. They have the common denominator (F_v) and $X_{(II)} + q_N + q_C = 1$, where 1 means F_v (Lysenko *et al.* 2020). If one of them increases, then the sum of two others will decrease and *vice versa*. It is advantageous to begin the analysis of PSII activity from nonphotochemical quenching.

Nonphotochemical quenching: In the control, both species showed similar dynamics of nonphotochemical quenching (Fig. 4S). Under Cd stress, barley plants demonstrated the tendency to decrease nonphotochemical quenching and a broader range of changes; maize plants demonstrated the tendency to increase nonphotochemical quenching and a narrower range of variation (Fig. 3). The lowest q_N values were found in barley; the highest q_N values were observed in maize (Fig. 4S). The changes observed can be referred to as neither a direct nor an indirect mechanism of Cd action.

At 80 µM Cd, q_N decreased (Fig. 3). The decrease was large in barley and very small in maize which corresponded to the large and small Cd contents in their chloroplasts (Lysenko *et al.* 2015). This decrease can be attributed to a direct Cd action. At 250 µM Cd, the effect was reversed. The level of nonphotochemical quenching increased at 250 µM Cd compared with 80 µM Cd; it was obvious in three cases (Fig. 3*B–D*). This reverse effect at 250 µM Cd cannot be ascribed to the changes of Cd content in the chloroplasts and a direct Cd action. The reversed tendency was dissimilar in barley and maize; hence, we have no reason to suggest an indirect effect due to the increasing general toxicity. However, the changes of nonphotochemical quenching (Fig. 3) were mirrored with the levels of closed PSII (Fig. 4); the latter can be explained (*see* below).

Cd treatment can change nonphotochemical quenching both up and down. It was observed in different studies (Burzyński and Żurek 2007, He *et al.* 2008, Lysenko *et al.* 2015, 2020) and even in a single experiment. The opposite Cd effect was obtained under different concentrations: q_N increased at 50 and 250 µM Cd, unchanged at 1 mM Cd, and decreased at 5 mM Cd (Geiken *et al.* 1998). At 20 µM and 80 µM Cd, NPQ decreased due to the reduction of fast relaxing component q_E; simultaneously, its slow-relaxing component q_I increased (Lysenko *et al.* 2015). In these studies, nonphotochemical quenching was presented as a single-point measurement after a light induction. The data in Fig. 3*A,B* shows nonlinear dynamics; we can describe different Cd effects by selecting particular points from these dynamics. It is favorable to show results as a dynamic process obtained with the use of different ALs; the Cd effect should be studied as a combination of IC and RLC or several ICs under different AL intensities.

Photochemical quenching: The decrease of nonphoto-chemical quenching retained more light energy in PSII. This extra energy is distributed between open $[X_{(II)}]$ and closed (q_C) PSII. The pattern of changes was diverse. In IC measured at AL of 128 µmol(photon) m^{-2} s^{-1}, the changes of nonphotochemical quenching influenced open PSII both up and down (Fig. 2*A,B*). In RLC, the decrease of q_N mostly increased closed PSII while the increase of q_N mainly resulted in the decrease of open PSII (Figs. 2*C,D*; 4*C,D*).

The balance between open and all (open + closed) PSII (q_P) was nearly unchanged in maize at 80 µM Cd; in other cases, q_P decreased (Fig. 2*E–H*). In barley under both Cd concentrations, q_P decreased due to q_C increase. During the first 40–120 s since the light induction, Cd treatment increased both $X_{(II)}$ (Fig. 2*A*) and q_C (Fig. 4*A*) whereas q_P remained unchanged (Fig. 2*E*); no q_P changing indicates that both $X_{(II)}$ and q_C increased proportionally to each other. Since 160 s, $X_{(II)}$ in the control was increasing and later reached the level of Cd-treated variants (Fig. 2*A*), while q_C in the control did not increase (Fig. 4*A*). The decreasing q_P in Cd-treated plants (Fig. 2*E*) reflects losing of difference in $X_{(II)}$ and persisting difference of q_C. In RLC, the impact of q_C was obvious (Figs. 2*C,G*; 4*C*). In maize at 250 µM Cd, q_P decreased due to $X_{(II)}$ decrease. The observed alterations of photochemically active PSII cannot be explained within the framework of this experimental model.

In barley plants, Cd stress accelerated the readaptation of the photochemical activity of PSII to light conditions. Cd-treated plants reached a stationary level faster than in the control (Fig. 2*A*). In maize plants at 80 µM Cd, the acceleration was very small (Fig. 2*B*). A similar accelerative effect was observed for PSI (*see* above). In barley plants, heat stress accelerated the restoration of $X_{(II)}$ during the first 2 min after AL induction (Lysenko *et al.* 2023). The accelerated readaptation of the photosystems to light conditions can be a general feature of abiotic stresses that were not observed before. This accelerative effect was more specific to barley young plants than to maize ones.

Acceptor-side limitation of PSII (q_C): The observed changes in closed PSII can be explained by a two-component mechanism. At 80 µM Cd, q_C changed in agreement with Cd accumulation in the chloroplasts.

Barley chloroplasts accumulated a large amount of Cd while maize chloroplasts accumulated a small portion of Cd (Lysenko *et al.* 2015). In IC under relatively low AL intensity, q_C increased slightly in barley and remained practically unchanged in maize (Fig. 4*A,B*). In RLC under rather high AL intensities, q_C demonstrated a large increase in barley plants and a small increase in maize plants (Fig. 4*C,D*). Thus, we can suppose a direct Cd effect on q_C at 80 μM Cd.

Increasing the concentration from 80 μM to 250 μM Cd reversed this effect. The level of q_C decreased at 250 μM compared with 80 μM Cd (Fig. 4); the decrease was similar in barley and maize (Fig. 8S, *supplement*). The concentration shift from 80 μM to 250 μM Cd induced diverse changes in Cd content in the chloroplasts and a similar increase of general toxicity in barley and maize plants (Lysenko *et al.* 2015). Thus, the similar decrease (Fig. 8S) should be referred to as an indirect effect of Cd at 250 μM. We hypothesize that the portion of closed PSII increased by a direct mechanism at 80 μM Cd; at 250 μM Cd, this effect was overcome *via* an indirect mechanism decreasing q_C.

Possible mechanisms: The direct inhibitory action of Cd on the oxygen-evolving complex of PSII is generally accepted. It was shown both *in vitro* (Bazzaz and Govindjee 1974, Sigfridsson *et al.* 2004) and *in vivo* (Baszyński *et al.* 1980). In barley chloroplasts, the quantity of Cd was sufficient to replace one of the four Mn in the oxygen-evolving complex (Lysenko *et al.* 2019). Artificial water-oxidizing complexes consisted of one, two, or four Mn atoms; some artificial Mn-catalysts comprised Cd^{2+} as the redox-inert ion stabilizing a crystal structure (reviewed in Najafpour *et al.* 2016). Therefore, we are unsure whether a single Cd/Mn substitution is capable of inhibiting the Mn_4CaO_5 cluster or not. Anyway, this mechanism cannot explain the changes in PSII activity observed in the current study (Figs. 1, 2, 3, 4).

Otherwise, the hypothesis of Cd/Cu substitution in plastocyanin (*see* above) explains the inhibition of electron transfer between the acceptor side of PSII and donor side of PSI. The bottleneck in electron traffic can increase the portion of PSII reaction centers limited (closed) at the acceptor side at 80 μM Cd that was masked with an indirect mechanism at 250 μM Cd.

Phosphate shortage can limit photosynthesis by restricting ATP synthesis (Sage and Kubien 2007). Suppressing ATP-synthase activity inhibits the unloading of ΔpH gradient and maintains a higher level of pH-dependent nonphotochemical quenching. In the late part of IC, increasing Cd concentration slowed down the decay of nonphotochemical quenching. In both species, the angles of q_N and NPQ decay slopes ranged similarly: control > 80 μM Cd > 250 μM Cd (Fig. 3*A,B*; Fig. 3S*A,B*). Consequently, an indirect Cd action inhibited the exhausting of ΔpH gradient, possibly, by limiting the ATP-synthase activity. Cd impact on inorganic phosphate in chloroplasts had not been studied. However, the phosphate shortage may be the indirect mechanism of Cd action that decreased q_C and overrode the direct

effect at 250 μM Cd (Fig. 8S). The next scheme can be hypothesized: phosphate shortage → ATP-synthase inhibition → slowdown of ΔpH exhaustion → increasing of nonphotochemical quenching → decreasing of light energy in PSII and portion of closed PSII (q_C).

The balance between the activities of PSI and PSII: We compared the photochemical activities of PSI [$Y_{(I)}$] and PSII [$X_{(II)}$] under illumination. After the light induction, the ratio $Y_{(I)}/X_{(II)}$ gradually increased in the control variants; the ratio reached a maximum in 2 min and further decreased slowly (Fig. 7*A,B*). Cd treatment accelerated the readaptation to light conditions in barley plants. The ratio $Y_{(I)}/X_{(II)}$ reached the steady-state level very fast (0.5 s), though this level was lower than in the control (Fig. 7*A*). This acceleration was specific to barley and Cd treatment (Fig. 7*A,B*). Under heat stress, $Y_{(I)}/X_{(II)}$ also increased faster during the first second since the light induction (Lysenko *et al.* 2023); however, this increase was smaller and observed in both barley and maize plants.

Cd treatment decreased the ratio $Y_{(I)}/X_{(II)}$ in barley plants in both IC and RLC (Fig. 7*A,C*). This means a larger inhibition of PSI compared with PSII that was concluded previously (Lysenko *et al.* 2020). A small decrease of $Y_{(I)}/X_{(II)}$ was revealed in maize at 80 μM Cd; the decrease was significant at some points of IC and RLC (Fig. 7*B,D*). However, $Y_{(I)}/X_{(II)}$ increased in maize at 250 μM Cd; it was observed in both IC and RLC (Fig. 7*B,D*). In this case, we should conclude that PSII was inhibited more than PSI.

In maize, the inhibitory effect of 250 μM Cd was similar in $Y_{(I)}$ and $X_{(II)}$; in many points, $Y_{(I)}$ was reduced more than $X_{(II)}$ (Fig. 9S, *supplement*). However, the values of $Y_{(I)}$ (Fig. 5*B,D*) were much larger than the values of $X_{(II)}$ (Fig. 2*B,D*); therefore, $Y_{(I)}$ was reduced proportionally smaller compared with $X_{(II)}$ (Fig. 7*B,D*). For leaves with single-type mesophyll chloroplasts, we have to follow proportional changes of $Y_{(I)}$ and $X_{(II)}$ that, probably, reflect some stoichiometry and/or relative activities of PSI and PSII. However, maize is a C4 plant with typical Kranz anatomy; these plants bear nearly equal amounts of mesophyll and bundle sheath cells in their leaves (Langdale 2011). Mesophyll cells include chloroplasts with both PSII and PSI; in NADP-ME type C4 plants, bundle sheath cells contain chloroplasts with PSI and no or very small activity of PSII (Turkan *et al.* 2018). In maize, PSII can be inhibited practically in mesophyll-type chloroplasts only. Was PSI inhibited in one or both types of chloroplasts?

We do not know the Cd content in bundle sheath cell chloroplasts. Our previous study was focused on mesophyll chloroplasts; therefore, the leaf homogenization was rather mild (Lysenko *et al.* 2015). The destruction of bundle sheath cells for chloroplast isolation requires a harder procedure (Jenkins and Boag 1985, Romanowska and Parys 2011). Therefore, we have to consider three possibilities. (*1*) In both types of chloroplasts, PSI activity decreased similarly; so, PSI was inhibited less than PSII in the mesophyll chloroplasts. (*2*) In the mesophyll chloroplasts, PSI and PSII were inhibited similarly while PSI remained unchanged in the bundle sheath cell chloroplasts. (*3*) In the mesophyll chloroplasts, PSI was

inhibited more than PSII; however, PSI activation in the bundle sheath cell chloroplasts compensated for it. The question of Cd action on processes in bundle sheath cell chloroplasts has not been previously addressed. Therefore, we cannot decide which of the variants is true.

Can we find an adaptive explanation for decreasing PSII activity in maize? A similar effect was observed under heat stress. Under the most severe conditions, $X_{(II)}$ decreased more than $Y_{(I)}$ which increased the ratio $Y_{(I)}/X_{(II)}$ in maize plants (Lysenko *et al.* 2023). Barley plants demonstrated no increase of $Y_{(I)}/X_{(II)}$ and died just after completing the experiment, while maize plants survived (Lysenko *et al.* 2023). These data interfere with considering large $X_{(II)}$ decrease under severe stress as an inhibitory process.

Plants with C_4 type of photosynthesis (including maize) have a lesser Rubisco content (Ku *et al.* 1979) and a smaller proportion of Rubisco oxygenase activity (Turkan *et al.* 2018) than C_3 plants. Elevating temperature enhances the impact of oxygenase activity by reducing Rubisco's affinity to CO_2 and increasing its affinity to O_2 (Laing *et al.* 1974). Cd treatment decreased Rubisco content (Pietrini *et al.* 2003, Lysenko *et al.* 2015). As a C_4 plant, maize features restricting PSII-dependent oxygen production and enhancing energy acquisition from the cyclic electron transport around PSI. Considering this, the adaptive explanation can be suggested as follows.

Under very severe stress (250 µM Cd, 46°C), maize plants upregulated nonphotochemical quenching (Fig. 3B,D) to restrict PSII activity (Fig. 2B,D), PSII-dependent oxygen production, and oxygenase activity of Rubisco. Restricting PSII-dependent O_2 production can increase ribulose-1,5-bisphosphate carboxylation and reduce both the production of toxic 2-phosphoglycolate and the waste of energy for its inactivation through the mechanism of photorespiration (Langdale 2011, Turkan *et al.* 2018). Under conditions of heavy stress, declining Rubisco oxygenase activity can be more advantageous compared with energy acquisition from PSII.

Balance between limitations of PSI and PSII: The ratio $q_C/Y_{(NA)}$ shows the balance of limitations at the acceptor sides of PSII (q_C) and PSI [$Y_{(NA)}$]. Half a second after the light induction, both limitations were large (Figs. 4A,B; 6E,F). In maize, both limitations were nearly equal (Fig. 8B inset); in barley, q_C was 15% smaller than $Y_{(NA)}$ while Cd treatment equalized both limitations (Fig. 8A inset). In 2 min, $q_C/Y_{(NA)}$ reached a peak followed by a decrease (Fig. 8A,B). In barley, Cd treatment accelerated reaching the peak, which was not specific to Cd (not shown). In maize, control plants demonstrated no peak.

In the controls, both limitations were approximately equal or q_C was a little larger than $Y_{(NA)}$ [$q_C/Y_{(NA)} \approx$ 1.0–1.3–1.5) (Fig. 8A–D). Under Cd treatment, q_C was mostly larger than $Y_{(NA)}$; the difference reached five times. At the steady-state level, q_C was two times larger than $Y_{(NA)}$ in barley (Fig. 8A). In most parts, the dynamics of $q_C/Y_{(NA)}$ (Fig. 8A–D) simply reflected the changes of q_C (Fig. 4). Therefore, the photochemical activity of PSII was not limited by Calvin–Benson cycle. In the controls, limitations

of the electron-transport chain and Calvin-Benson cycle were balanced; in Cd-treated plants, limitations of the electron-transport chain prevailed.

The ratio $q_C/Y_{(ND)}$ compares limitations between the acceptor side of PSII (q_C) and the donor side of PSI [$Y_{(ND)}$]. It is a tool for studying the fragment of the electron-transfer chain including plastoquinone pool, cytochrome b_6/f, and plastocyanin.

Solely at the beginning of the curves, we observed $q_C > Y_{(ND)}$ or $q_C \approx Y_{(ND)}$; in RLC, this effect was less pronounced (Fig. 8E–H). In most parts of the curves, q_C was smaller than $Y_{(ND)}$. Consequently, this segment of the electron-transport chain was limited mostly to the donor side of PSI.

Cd treatment increased the ratio $q_C/Y_{(ND)}$ in barley, mostly unchanged it in maize at 80 µM Cd, and decreased it in maize at 250 µM Cd (Fig. 8E–H; Fig. 6S). The changes in both ratios $q_C/Y_{(NA)}$ and $q_C/Y_{(ND)}$ cannot be explained within the framework of this experiment.

We found short quasi-stationary levels in $q_C/Y_{(ND)}$ dynamics (Fig. 6S). The values of quasi-stationary levels varied from 0.2 to 0.65 [$q_C < Y_{(ND)}$]. In most cases, one variant showed equal values of quasi-stationary levels in both IC and RLC. In a variant, IC and RLC reached equal quasi-stationary levels in similar (Fig. 6SB) or different times (Fig. 6SA). The quasi-stationary levels were found in actively changing segments of q_C and $Y_{(ND)}$ dynamics; some examples are shown in Fig. 10S (*supplement*). In IC, the quasi-stationary levels were followed by the increases due to further decreases of $Y_{(ND)}$ (Fig. 6A,B). In RLC, the quasi-stationary levels were followed by the decreases mostly due to the decreases of q_C (Fig. 4C,D) because of the corresponding increases of nonphotochemical quenching (Fig. 3C,D). It is interesting to investigate $q_C/Y_{(ND)}$ quasi-stationary levels more in future studies.

References

Baker A.J.M.: Accumulators and excluders – strategies in response of plants to heavy metals. – J. Plant Nutr. **3**: 643-654, 1981.

Baryla A., Carrier P., Franck F. *et al.*: Leaf chlorosis in oilseed rape plants (*Brassica napus*) grown on cadmium-polluted soil: causes and consequences for photosynthesis and growth. – Planta **212**: 696-709, 2001.

Baszyński T., Wajda L., Król M. *et al.*: Photosynthetic activities of cadmium-treated tomato plants. – Physiol. Plantarum **48**: 365-370, 1980.

Bazzaz M.B., Govindjee: Effects of cadmium nitrate on spectral characteristics and light reactions of chloroplasts. – Environ. Lett. **6**: 1-12, 1974.

Bigalke M., Ulrich A., Rehmus A., Keller A.: Accumulation of cadmium and uranium in arable soils in Switzerland. – Environ. Pollut. **221**: 85-93, 2017.

Bilger W., Björkman O.: Role of the xanthophyll cycle in photoprotection elucidated by measurements of light-induced absorbance changes, fluorescence and photosynthesis in leaves of *Hedera canariensis*. – Photosynth. Res. **25**: 173-185, 1990.

Burzyński M., Żurek A.: Effects of copper and cadmium on photosynthesis in cucumber cotyledons. – Photosynthetica

45: 239-244, 2007.

Ci D., Jiang D., Wollenweber B. *et al.*: Cadmium stress in wheat seedlings: growth, cadmium accumulation and photosynthesis. – Acta Physiol. Plant. **32**: 365-373, 2010.

Dias M.C., Monteiro C., Moutinho-Pereira J. *et al.*: Cadmium toxicity affects photosynthesis and plant growth at different levels. – Acta Physiol. Plant. **35**: 1281-1289, 2013.

Díaz-Moreno I., Díaz-Quintana A., De la Rosa M.A., Ubbink M.: Structure of the complex between plastocyanin and cytochrome *f* from the cyanobacterium *Nostoc* sp. PCC 7119 as determined by paramagnetic NMR: The balance between electrostatic and hydrophobic interactions within the transient complex determines the relative orientation of the two proteins. – J. Biol. Chem. **280**: 18908-18915, 2005.

Gaillardet J., Viers J., Dupré B.: Trace elements in river waters. – In: Holland H.D., Turekian K.K. (ed.): Treatise on Geochemistry. Pp. 225-272. Pergamon, 2003.

Geiken B., Masojídek J., Rizzuto M. *et al.*: Incorporation of [^{35}S] methionine in higher plants reveals that stimulation of the D1 reaction centre II protein turnover accompanies tolerance to heavy metal stress. – Plant Cell Environ. **21**: 1265-1273, 1998.

Genty B., Briantais J.-M., Baker N.R.: The relationship between the quantum yield of photosynthetic electron transport and quenching of chlorophyll fluorescence. – BBA-Gen. Subjects **990**: 87-92, 1989.

Havaux M.: Short-term responses of photosystem I to heat stress: Induction of a PS II-independent electron transport through PS I fed by stromal components. – Photosynth. Res. **47**: 85-97, 1996.

He J.-Y., Ren Y.-F., Zhu C. *et al.*: Effect of Cd on growth, photosynthetic gas exchange, and chlorophyll fluorescence of wild and Cd-sensitive mutant rice. – Photosynthetica **46**: 466-470, 2008.

Jenkins C.L.D., Boag S.: Isolation of bundle sheath cell chloroplasts from the NADP-ME type C$_4$ plant *Zea mays*: Capacities for CO$_2$ assimilation and malate decarboxylation. – Plant Physiol. **79**: 84-89, 1985.

Jigyasu D.K., Singh M., Singh S. *et al.*: Trace element mobility, regional significance and global implication of Gomati river basin, northern India. – SN Appl. Sci. **2**: 1456, 2020.

Kalaji H.M., Schansker G., Ladle R.J. *et al.*: Frequently asked questions about *in vivo* chlorophyll fluorescence: practical issues. – Photosynth. Res. **122**: 121-158, 2014.

Klaus A.A., Lysenko E.A., Kholodova V.P.: Maize plant growth and accumulation of photosynthetic pigments at short- and long-term exposure to cadmium. – Russ. J. Plant Physiol. **60**: 250-259, 2013.

Klughammer C., Schreiber U.: An improved method, using saturating light pulses, for the determination of photosystem I quantum yield via P700$^+$-absorbance changes at 830 nm. – Planta **192**: 261-268, 1994.

Klughammer C., Schreiber U.: Saturation Pulse method for assessment of energy conversion in PSI. – PAM Appl. Notes **1**: 11-14, 2008.

Ku M.S.B., Schmitt M.R., Edwards G.E.: Quantitative determination of RuBP carboxylase–oxygenase protein in leaves of several C$_3$ and C$_4$ plants. – J. Exp. Bot. **30**: 89-98, 1979.

Kumar A., Subrahmanyam G., Mondal R. *et al.*: Bio-remediation approaches for alleviation of cadmium contamination in natural resources. – Chemosphere **268**: 128855, 2021.

Laing W.A., Ogren W.L., Hageman R.H.: Regulation of soybean net photosynthetic CO$_2$ fixation by the interaction of CO$_2$, O$_2$ and ribulose 1,5-diphosphate carboxylase. – Plant Physiol. **54**: 678-685, 1974.

Langdale J.A.: C$_4$ cycles: past, present, and future research on C$_4$ photosynthesis. – Plant Cell **23**: 3879-3892, 2011.

Lin Y.-F., Aarts M.G.M.: The molecular mechanism of zinc and cadmium stress response in plants. – Cell Mol. Life Sci. **69**: 3187-3206, 2012.,

Lysenko E.A.: Application of fast light-readapted plants for measurement of chlorophyll fluorescence and P$_{700}$ light absorption with the RLC method. – Photosynthetica **59**: 245-255, 2021.

Lysenko E.A., Klaus A.A., Kartashov A.V., Kusnetsov V.V.: Distribution of Cd and other cations between the stroma and thylakoids: a quantitative approach to the search for Cd targets in chloroplasts. – Photosynth. Res. **139**: 337-358, 2019.

Lysenko E.A., Klaus A.A., Kartashov A.V., Kusnetsov V.V.: Specificity of Cd, Cu, and Fe effects on barley growth, metal contents in leaves and chloroplasts, and activities of photosystem I and photosystem II. – Plant Physiol. Biochem. **147**: 191-204, 2020.

Lysenko E.A., Klaus A.A., Pshybytko N.L., Kusnetsov V.V.: Cadmium accumulation in chloroplasts and its impact on chloroplastic processes in barley and maize. – Photosynth. Res. **125**: 291-303, 2015.

Lysenko E.A., Kozuleva M.A., Klaus A.A. *et al.*: Lower air humidity reduced both the plant growth and activities of photosystems I and II under prolonged heat stress. – Plant Physiol. Biochem. **194**: 246-262, 2023.

Mahajan M., Gupta P.K., Singh A. *et al.*: A comprehensive study on aquatic chemistry, health risk and remediation techniques of cadmium in groundwater. – Sci. Total Environ. **818**: 151784, 2022.

Najafpour M.M., Renger G., Hołyńska M. *et al.*: Manganese compounds as water-oxidizing catalysts: From the natural water-oxidizing complex to nanosized manganese oxide structures. – Chem. Rev. **116**: 2886-2936, 2016.

Pan J., Plant J.A., Voulvoulis N. *et al.*: Cadmium levels in Europe: implications for human health. – Environ. Geochem. Health **32**: 1-12, 2010.

Pfündel E.E., Klughammer C., Meister A., Cerovic Z.G.: Deriving fluorometer-specific values of relative PSI fluorescence intensity from quenching of F_0 fluorescence in leaves of *Arabidopsis thaliana* and *Zea mays*. – Photosynth. Res. **114**: 189-206, 2013.

Pietrini F., Iannelli M.A., Pasqualini S., Massacci A.: Interaction of cadmium with glutathione and photosynthesis in developing leaves and chloroplasts of *Phragmites australis* (Cav.) Trin. ex Steudel. – Plant Physiol. **133**: 829-837, 2003.

Romanowska E., Parys E.: Mechanical isolation of bundle sheath cell strands and thylakoids from leaves of C$_4$ grasses. – In: Carpentier R. (ed.): Photosynthesis Research Protocols. Methods in Molecular Biology. Vol. 684. Pp. 327-337. Humana Press, Totowa 2011.

Rumeau D., Peltier G., Cournac L.: Chlororespiration and cyclic electron flow around PSI during photosynthesis and plant stress response. – Plant Cell Environ. **30**: 1041-1051, 2007.

Sage R.F., Kubien D.S.: The temperature response of C$_3$ and C$_4$ photosynthesis. – Plant Cell Environ. **30**: 1086-1106, 2007.

Schreiber U., Schliwa U., Bilger W.: Continuous recording of photochemical and nonphotochemical chlorophyll fluorescence quenching with a new type of modulation fluorometer. – Photosynth. Res. **10**: 51-62, 1986.

Seregin I.V., Ivanov V.B.: Physiological aspects of cadmium and lead toxic effects on higher plants. – Russ. J. Plant Physiol. **48**: 523-544, 2001.

Shi G.R., Cai Q.S.: Photosynthetic and anatomic responses of peanut leaves to cadmium stress. – Photosynthetica **46**: 627-630, 2008.

Siedlecka A., Baszyński T.: Inhibition of electron flow around photosystem I in chloroplasts of Cd-treated maize plants is due to Cd-induced iron deficiency. – Physiol. Plantarum **87**: 199-202, 1993.

Sigfridsson K.G.V., Bernát G., Mamedov F., Styring S.: Molecular interference of Cd^{2+} with Photosystem II. – BBA-Bioenergetics **1659**: 19-31, 2004.

Tang L., Ying R.-R., Jiang D. *et al.*: Impaired leaf CO_2 diffusion mediates Cd-induced inhibition of photosynthesis in the Zn/Cd hyperaccumulator *Picris divaricata*. – Plant Physiol. Biochem. **73**: 70-76, 2013.

Turkan I., Uzilday B., Dietz K.-J. *et al.*: Reactive oxygen species and redox regulation in mesophyll and bundle sheath cells of C_4 plants. – J. Exp. Bot. **69**: 3321-3331, 2018.

van Kooten O., Snel J.F.H.: The use of chlorophyll fluorescence nomenclature in plant stress physiology. – Photosynth. Res. **25**: 147-150, 1990.

Yamane Y., Shikanai T., Kashino Y. *et al.*: Reduction of Q_A in the dark: Another cause of fluorescence F_o increases by high temperatures in higher plants. – Photosynth. Res. **63**: 23-34, 2000.

Zou M., Zhou S., Zhou Y. *et al.*: Cadmium pollution of soil-rice ecosystems in rice cultivation dominated regions in China: A review. – Environ. Pollut. **280**: 116965, 2021.